

Methane Conversion to Methanol Using Au/ZSM-5 is Promoted by Carbon

Jingxian Cao, Richard J. Lewis, Guodong Qi, Donald Bethell, Mark J. Howard, Brian Harrison, Bingqing Yao, Qian He, David J. Morgan, Fenglou Ni, Pankaj Sharma, Christopher J. Kiely, Xu Li, Feng Deng, Jun Xu,* and Graham J. Hutchings*



Cite This: *ACS Catal.* 2023, 13, 7199–7209



Read Online

ACCESS |

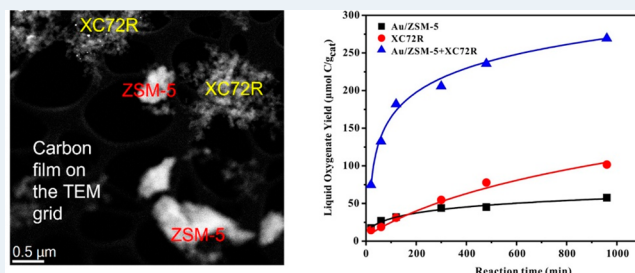
Metrics & More

Article Recommendations

Supporting Information

ABSTRACT: The oxidation of methane using molecular oxygen as the terminal oxidant, over a Au/ZSM-5 catalyst, has been previously shown to produce methanol and acetic acid as products. We now show that this reaction is significantly enhanced by the addition of a range of carbon additives. Isotopic ^{13}C -labeled studies and corresponding investigation into the activity of the carbon materials alone reveal that nearly all the methanol produced is derived from methane oxidation, with a negligible contribution attributed to the carbon additives, while further study identified carbon as the primary source of acetic acid, which was observed as a minor product. Gas phase CO is not observed as a product in the reaction of Au/ZSM-5 with $\text{CH}_4 + \text{O}_2$, and in reactions with added CO, not all the CO is converted. We, therefore, conclude that the effect observed with the carbon additive is not due to the in situ production of gas phase CO as a reaction intermediate. Rather, we postulate that the effect derives from the oxidation of the surface of the carbon in the aqueous reaction mixture and the interaction of the oxidized carbon surface with Au/ZSM-5. The reactivity of carbon in this reaction at 240 °C is unexpected, and the presence of water is required to observe the effect.

KEYWORDS: methane oxidation, low temperature, liquid phase, Au nanoparticles, carbon



INTRODUCTION

The selective oxidation of methane to methanol or other valuable oxygenated products represents, for many, a grand challenge in catalysis. Indeed, it has often been considered a dream reaction for industrial catalysis, and more recently it can be considered to be of potential benefit to valorize emissions of natural gas that are currently flared.¹ In recent years, a major focus for the selective oxidation of methane has been placed on the use of lower reaction temperatures (<300 °C) in order to suppress nonselective oxidation pathways. A notable step forward in selective methane oxidation was demonstrated by Periana and co-workers, who showed that electrophilic Hg and Pt-complexes could oxidize methane in oleum,^{2,3} forming methyl hydrogen sulfate which could subsequently be separately hydrolyzed to generate methanol and sulfuric acid. While these schemes would require multiple process steps, this pioneering work showed that by careful reaction and catalyst design, the reaction could be achieved.

Recently interest has shifted to using metal-exchanged zeolitic materials as catalysts. Notable examples include Fe-ZSM-5^{4–7} and FeCu-ZSM-5^{8,9} which are able to offer high selectivity toward CH_3OH when using either N_2O or H_2O_2 as oxidant. Alternatively, Cu-mordenite¹⁰ and Rh-ZSM-5^{11,12} are both able to produce CH_3OH with O_2 when using CO as a co-reductant. AuPd alloys, either immobilized onto a support such

as ZSM-5¹³ or unsupported, also demonstrate activity when using H_2O_2 .¹⁴ However, notably for all these examples, no selective oxygenate products are formed with O_2 alone, and hence either a more active oxidant (H_2O_2 , N_2O) or a reducing agent (H_2 , CO) is required.

Cu-mordenite catalysts can be operated in a two-stage catalytic cycle to form CH_3OH .^{15–17} In this case, an oxidized Cu species is reacted with CH_4 forming a surface methoxyl which is subsequently extracted at a lower temperature with water. Subsequently, van Bokhoven and co-workers demonstrated¹⁸ that Cu-mordenite can oxidize CH_4 with a continuous flow of H_2O to produce methanol; however, this reaction was stoichiometric. Roman-Leshkov and co-workers^{19,20} have shown that Cu-mordenite can oxidize methane in a continuous flow of H_2O and O_2 with a closed catalytic cycle. In addition, Koishybay and Shantz²¹ have demonstrated that

Received: March 17, 2023

Revised: April 27, 2023

when using Cu-SSZ-13 as a catalyst, it is H₂O that is the source of the oxygen in the synthesized methanol.

Gold catalysts have been found to have exceptional activity in selective oxidation,²² and most recently we have reported²³ that the oxidation of CH₄ using O₂ can be achieved in the absence of a co-reductant (H₂ or CO) in a closed catalytic cycle when using Au supported on ZSM-5 with high selectivity to oxygenated products achieved at reaction temperatures between 120 and 240 °C. In this initial study, we showed the active site for the reaction was gold nanoparticles (≥ 6 nm in diameter) supported on the exterior surface of the zeolite. Most interestingly, acetic acid was observed as the main selective oxidation product, which is in contrast to all previous studies where methanol is the main product. Using detailed isotopic studies (D and ¹³C), we confirmed that the mechanism by which acetic acid was formed involved a surface coupling reaction between two C₁ species. The formation of acetic acid was enhanced by the addition of CO, and in this case, the methyl carbon of the acetic acid was derived from methane and the carboxyl carbon was mostly derived from the cofed CO. With these earlier studies in mind,²³ in particular those which utilize CO as a co-reductant, we now investigate the effect of the addition of a range of carbon sources on the oxidation of methane with O₂ using Au/ZSM-5 as a catalyst and demonstrate that the addition of carbon has a marked and unexpected effect on the observed catalysis.

EXPERIMENTAL METHODS

Note on Safe Operation of Experiments. When conducting catalytic oxidation, it is important to ensure that reaction conditions are such that the experiments are not conducted in the explosion region. For methane oxidation, Cooper and Wiezevich²⁴ have shown that experiments conducted with $\leq 14\%$ O₂ even at elevated temperature and pressure are outside the explosive region, and this is the case in the work reported here.

Catalyst Preparation. Materials. NH₄-ZSM-5 zeolite (SiO₂/Al₂O₃ = 25) was obtained from Nankai University Catalyst Co., Ltd. Gold(III) chloride trihydrate (HAuCl₄·3H₂O, $\geq 49.0\%$ Au basis) was purchased from Merck. Aqueous ammonia (25–28%), sodium carbonate (99.8%), sodium hydroxide ($\geq 96\%$) and hydrochloric acid (37%) were obtained from Sinopharm Chemical Reagent Co., Ltd. Methane (99.999%) was obtained from Dalian Special Gases Co., Ltd. Nitrogen (99.999%) and oxygen (99.999%) were obtained from Wuhan Huaxing Industrial Gas Co., Ltd. ¹³CH₄ (¹³C, 99%, 99.9% chemical purity) was purchased from Cambridge Isotope Laboratories, Inc. Poly(vinyl alcohol) (PVA) (MW $\approx 10,000$, 80% hydrolyzed) was obtained from Aldrich.

Several carbons were used in this experimental program, including XC72R (Cabot) and Black Pearls (Cabot), in addition to a series of functionalized graphitic carbons (Haydale) and oxidized Norit ROX 0.8-based carbons. The naming convention used for the functionalized graphitic carbons is based on the oxygen/carbon ratio as determined by XPS. For the Norit ROX 0.8-based carbons, the nomenclature refers to the carbon:potassium permanganate ratio utilized in the oxidation of these materials, so for the sample termed Norit ROX 1:0.5, the carbon (5g) was modified by the presence of potassium permanganate (2.5 g).

With the exception of the Norit ROX 0.8-based carbons, all materials and reagents were used directly without purification.

The procedure to modify the Norit ROX 0.8 carbons is outlined below.

Preparation of Oxidized Carbons. Ground activated carbon (AC) was oxidized according to a previously reported modified Hummers method.^{25,26} AC (5 g) was added to a mixture of concentrated sulfuric (88 mL) and nitric acid (28 mL) under vigorous stirring and allowed to cool to 10 °C in an ice bath. Nitric acid was used in place of sodium nitrate to eliminate sodium contamination from the final material. Potassium permanganate (2.5 or 7.5 g) was added stepwise over a period of 2 h with the temperature maintained below 10 °C. The mixture was then allowed to reach room temperature over a period of 4 h, followed by heating to 35 °C for 30 min. Deionized water (250 mL) was added, causing the temperature to rise to 70 °C. After 15 min, a further portion of deionized water (1 L) was added, followed by the addition of 3% hydrogen peroxide to quench the residual oxidant. The mixture was allowed to settle overnight after which the sample was separated and washed repeatedly via centrifugation until a neutral pH was obtained. The sample was finally dried at 30 °C under vacuum for 16 h. An analogous water-washed sample was also prepared; AC (5.0 g) was added to 1L of water and stirred vigorously for 6 h. The sample was then separated via centrifugation and dried at 30 °C under vacuum for 16 h.

Catalyst Synthesis. Prior to Au deposition, the as-received zeolitic material (NH₄-ZSM-5) was first exposed to an oxidative heat treatment (450 °C at 3 °C/min for 6 h).

0.5 wt % Au loaded catalysts were prepared by a deposition-precipitation method using aqueous ammonia as the base to control the pH value.²³ This method was used to ensure the catalysts prepared contained no adventitious carbon impurities. Typically, ZSM-5 (3.0 g) was dispersed in deionized water (200 mL) and was mixed with a known amount of HAuCl₄ (6.0 mmol/L, aqueous solution) with stirring at 600 rpm. An appropriate amount of 2.5 wt % aqueous ammonia solution was slowly added until pH 6 was achieved. This step took more than 30 min at room temperature. The resulting solution was aged (60 °C, 2 h) with stirring (600 rpm), and the final pH value was around 5. The solid was collected by filtration, washed with deionized water, dried in air (60 °C, 16 h) and calcined (static air, 90 min, 240 °C, 3 °C/min). All the Au-ZSM-5 samples had 0.5 wt % Au loading unless otherwise stated.

An additional catalyst was prepared in an analogous manner in the presence of PVA. An aqueous solution of PVA (PVA (1.0 g) in water (50 mL)) was mixed with ZSM-5 (3.0 g) dispersed in deionized water (150 mL). The subsequent procedure was identical to that described above for the Au/ZSM-5 catalyst, with the resulting catalyst denoted PVA-Au-ZSM-5.

Catalyst Characterization. XPS was performed on a Thermo Fisher Scientific K-alpha⁺ photoelectron spectrometer. Samples were mounted in small recesses within the Thermo Scientific copper powder plate. Samples were analyzed using a microfocused monochromatic aluminum X-ray source operating at 72 W (6 mA \times 12 kV) using the 400 μ m spot option, which is an elliptical area of approximately 400 μ m \times 600 μ m. Data were recorded at pass energies of 200 eV for survey scans and 50 eV for high-resolution scans with 1 and 0.1 eV step sizes, respectively. Where required, charge compensation of the sample was achieved using a combination of both low-energy electrons and argon ions, which results in a C(1s) energy for the carbon support of 284.5 eV, typical of graphitic-like

Table 1. Comparison of Methane Oxidation Using Au/ZSM-5 and PVA-Au/ZSM-5 Catalysts^a

Catalyst	Reactants CH ₄ , O ₂ , CO (bar)	Productivity (μmol/g _{cat})					CO ₂	Oxygenate selectivity (%)	Methanol Sselectivity in liquid (%)	Oxygenate productivity (μmol/g _{cat})
		Methanol	Methyl hydroperoxide	Acetic acid	Peracetic acid					
Au/ZSM-5	20.7, 3.5, 0	9.72	0.6	7.5	3.3	20.0	61.4	30.5	21.1	
PVA-Au/ZSM-5	20.7, 3.5, 0	21.3	2.0	50.7	5.5	93.6	59.2	15.7	79.5	

^aReaction conditions: Catalyst (0.1 g), H₂O (15 mL), 240 °C, 2 h, CH₄ (20.7 bar) and O₂ (3.5 bar), 1000 rpm.

Table 2. Influence of Carbon on Methane Oxidation over Au/ZSM-5 Catalyst^a

Entry	Carbon additive	Productivity (μmol/g _{cat})					CO ₂	Oxygenate selectivity (%)	Methanol selectivity in liquid (%)	Oxygenate productivity (μmol/g _{cat})
		Methanol	Methyl hydroperoxide	Acetic acid	Peracetic acid					
1	Au/ZSM-5	9.7	0.6	7.48	3.29	20.0	61.4	30.5	21.1	
2	Au/ZSM-5+Norit Rox 0.8	111	0	14.9	0	2155	6.13	78.8	126	
3	Norit Rox 0.8*	4.83	b.d.	9.81	b.d.	1805	1.34	19.76	14.6	
4	Au/ZSM-5+Norit Rox washed	93.1	0	28.6	0	3555	4.06	61.9	122	
5	Au/ZSM-5+Norit Rox 1:0.5	68.4	0	98.0	0	5108	4.92	25.9	166	
6	Au/ZSM-5+Norit Rox 1:1.5	53.9	0	114	0	4830	5.50	19.2	167	
7	Norit Rox 1:1.5*	9.38	b.d.	77.8	b.d.	3158	4.96	5.69	87.1	
8	Au/ZSM-5+ Graphitic O/C = 0.067	82.4	4.61	83.4	3.29	2111	10.9	31.7	174	
9	Au/ZSM-5+ Graphitic O/C = 0.186	120	5.66	144	7.95	2387	15.3	27.9	278	
10	Au/ZSM-5+ Graphitic O/C = 0.170	177	4.52	183	9.04	3623	13.53	31.3	374	
11	Graphitic O/C = 0.170*	5.87	2.15	121	2.79	2378	9.67	2.31	131	
12	Au/ZSM-5+ Graphitic O/C = 0.183	148	3.78	162	4.64	3240	13.0	30.5	318	
13	Au/ZSM-5+ Graphitic O/C = 0.185	117	3.50	114	4.23	2350	13.22	32.7	239	
14	Au/ZSM-5+Black Pearls	159	b.d.	20.4	b.d.	2390	7.7	79.6	180	
15	Au/ZSM-5+XC72R	156	b.d.	13.0	b.d.	784	18.8	85.7	169	
16	XC72R*	9.58	b.d.	4.62	b.d.	501	3.62	50.9	14.2	

^aReaction conditions: Au/ZSM-5 (0.1 g), carbon (0.08 g), H₂O (15 mL), 240 °C, 2 h, 1000 rpm. b.d.: below detection limit. * denotes the use of carbon (0.08 g) only, in the absence of the Au/ZSM-5 catalyst. These carbons were chosen as they represent a range of oxygen functionality.

carbons. Data analysis was performed in CasaXPS (v. 2.3.25)²⁷ using transmission corrected data converted from the Thermo Advantage software. Peak areas were corrected using Scofield cross sections²⁸ after removal of a Shirley-type background. Electron mean free paths are calculated using the TPP-2 M equation.²⁹

N₂-physisorption analyses were performed on a Micromeritics 3Flex instrument at 77 K. Prior to analysis, ca. 0.15 g of the sample was degassed at 200 °C under a vacuum for 24 h. Free space was measured postanalysis using He. The Brunauer–Emmett–Teller model was used to determine the specific surface area under the relative pressure range of 0.05–0.30. Total pore volume (V_{pore}) was estimated from the adsorption branch of the isotherm at $P/P_0 = 0.98$. The microporous volume (V_{micro}) was estimated from the t-plot. Pore volume distribution was estimated using the BJH model.

Au content in the catalysts was determined by inductively coupled plasma optical emission spectrometry (ICP-OES) using an Agilent 700 spectrometer.

STEM high-angle annular dark-field (HAADF) imaging was performed at the National University of Singapore, using an aberration-corrected JEOL ARM200CF microscope equipped with a cold field-emission gun operating at 200 kV.

The carbon content of PVA-Au-ZSM-5 was determined by using thermogravimetric analysis (TGA) on a Mettler DSC3+ instrument. The adsorbed water was removed by heating the sample in a nitrogen flow at temperature below 140 °C. In the temperature range from 140 to 800 °C, the gas flow was switched to zero-air for a complete degradation of the residual carbon. The carbon content was determined by measuring the weight loss under the zero-air condition.

Catalyst Testing. Methane oxidation with oxygen was carried out in a 25 mL stainless steel Parr autoclave reactor. In general, the catalyst (0.1 g), carbon (typically 0.1 g) and H₂O (15 mL) were transferred into the reactor, which was subsequently sealed and purged with N₂ for >30 min at 2 bar pressure to remove dissolved gases. After purging three times with methane, the reactor was pressurized with a gas mixture of methane and oxygen. The total pressure was set at

Table 3. Control Reactions for Methane Oxidation Using XC72R and Au/ZSM-5^a

Entry	Catalyst	Reactants CH ₄ , O ₂ , N ₂ (bar)	Productivity (μmol/g _{cat})				CO ₂	Oxygenate selectivity (C _{mol} %)	Methanol selectivity in liquid (%)	Oxygenate productivity (μmol/g _{cat})
			Methanol	Methyl hydro peroxide	Acetic acid	Peracetic acid				
1	XC72R	0, 0, 24.2	0.1	b.d.	0.5	b.d.	8.5	11.5	9.1	0.6
2	XC72R	24.2, 0, 0	1.5	b.d.	0.9	b.d.	6.0	35.5	45.5	2.4
3	XC72R	0, 3.5, 20.7	b.d.	b.d.	b.d.	b.d.	716	–	–	0
4	Au/ZSM-5 + XC72R	0, 3.5, 20.7	b.d.	b.d.	12.5	b.d.	830	2.92	–	12.5
5	XC72R	20.7, 3.5, 0	9.58	b.d.	4.62	b.d.	501	3.62	50.9	14.2

^aReaction conditions: Entries 1–3: XC72R (0.1 g); entry 4: Au/ZSM-5 (0.1 g), XC72R (0.08 g); and entry 5: XC72 (0.08 g) H₂O (15 mL), 240 °C, 2 h, 1000 rpm. b.d.: below detection limit.

Table 4. CH₄ Oxidation in the Presence of XC72R and Au/ZSM-5^a

Entry	Catalyst	Productivity (μmol/g _{cat})					XC72R conversion (%)	Oxygenate selectivity (%)	Methanol selectivity in liquid (%)	Oxygenate productivity (μmol/g _{cat})
		Methanol	Methyl hydroperoxide	Acetic acid	Peracetic acid	CO ₂				
1	Au/ZSM-5	9.72	0.6	7.5	3.3	20.0	0	61.4	30.4	21.1
2	Au/ZSM-5+ XC72R (0.005 g)	28.1	1.4	9.8	0	70.7	0.7	61.4	30.4	21.1
3	Au/ZSM-5+ XC72R (0.02 g)	43.4	0	7.3	0	142	0.3	41.0	57.2	39.2
4	Au/ZSM-5+ XC72R (0.06 g)	95.8	b.d.	12.1	b.d.	357	0.3	28.9	74.8	50.7
5	Au/ZSM-5+ XC72R (0.08 g)	156	b.d.	13.0	b.d.	784	0.5	25.2	79.8	107
6	Au/ZSM-5+ XC72R (0.1 g)	167	b.d.	16.0	b.d.	895	0.4	18.8	85.7	169
7	Au/XC72R (0.08 g)	81.7	b.d.	7.7	b.d.	651	0.3	18.2	83.9	183

^aReaction conditions: Catalyst (0.1 g), XC72R (0–0.1 g), H₂O (15 mL), 240 °C, 2 h, CH₄ (20.7 bar) and O₂ (3.5 bar), 1000 rpm. b.d. below detection limit.

24.2 bar with varied methane and oxygen partial pressures measured at room temperature. The mixture was initially stirred at 1000 rpm for 10 min at room temperature and the pressure remained constant at around 24 bar. The reactor was then heated to the required reaction temperature and stirred at 1000 rpm for a predetermined period, typically 2 h. After this time, the stirring was stopped, and the reactor cooled in ice water to a temperature below 10 °C in order to minimize the loss of volatile products. Gaseous reagents in the head space of the reactor were collected for analysis in a gas sampling bag at the end of a reaction. Liquid products were sampled using a glass syringe with Teflon filter head and analyzed via NMR. For reactions involving the addition of carbon, the specified carbon was added together with the catalyst at the start of the reaction.

In all cases, reactions were run multiple times over multiple batches of catalyst, with the data presented as an average of these experiments. Catalytic activity was determined to be consistent within ±5% on the basis of multiple reactions.

Isotopic Tracer Experiments. To trace the fate of carbon atoms from methane and to distinguish their fate from that of the added carbon, ¹³C-labeled CH₄ was used in the reaction with oxygen. A high-sensitivity NMR CryoProbe on a Bruker Avance-600 liquid NMR spectrometer was employed to analyze the liquid products obtained from the isotopic tracing experiments. ¹H NMR spectra were recorded using a water suppression pulse sequence. The gas composition after the reaction was analyzed by a Hiden HPR-20 mass spectrometer.

RESULTS AND DISCUSSION

Initially we investigated the performance of a Au/ZSM-5 catalyst toward the oxidation of methane using a catalyst prepared via deposition precipitation (Table 1). As we have reported previously,²³ methane is oxidized to both C₁ and C₂ products. The Au/ZSM-5 catalyst was prepared using deposition precipitation in the absence of any sources of adventitious carbon, since the presence of such carbon could mask the effects we sought to observe for methane oxidation. Next, we prepared a similar Au/ZSM-5 catalysts using a sol-immobilization procedure, in order to determine the effect of a catalyst prepared with the addition of a source of carbon in the form of PVA (PVA-Au/ZSM-5). TGA analysis revealed that this catalyst contained approximately 64 mg/g of adventitiously added carbon (Figure S1). Subsequent determination of the performance of the PVA-Au/ZSM-5 catalyst toward methane oxidation (Table 1) revealed that the presence of the added carbon in the PVA-Au/ZSM-5 catalyst led to a significant enhancement in the yield of the oxygenated products as well as CO₂. As PVA is an oxygenate, the enhanced formation of such products is not a surprising observation and is in keeping with our prior studies into Fe-based catalysts comprising organic ligands for methane oxidation, where the presence of the ligand led to a false impression of any underlying methane conversion.³⁰ However, this interesting observation led us to investigate the addition of carbon in a controlled way to this catalyzed reaction.

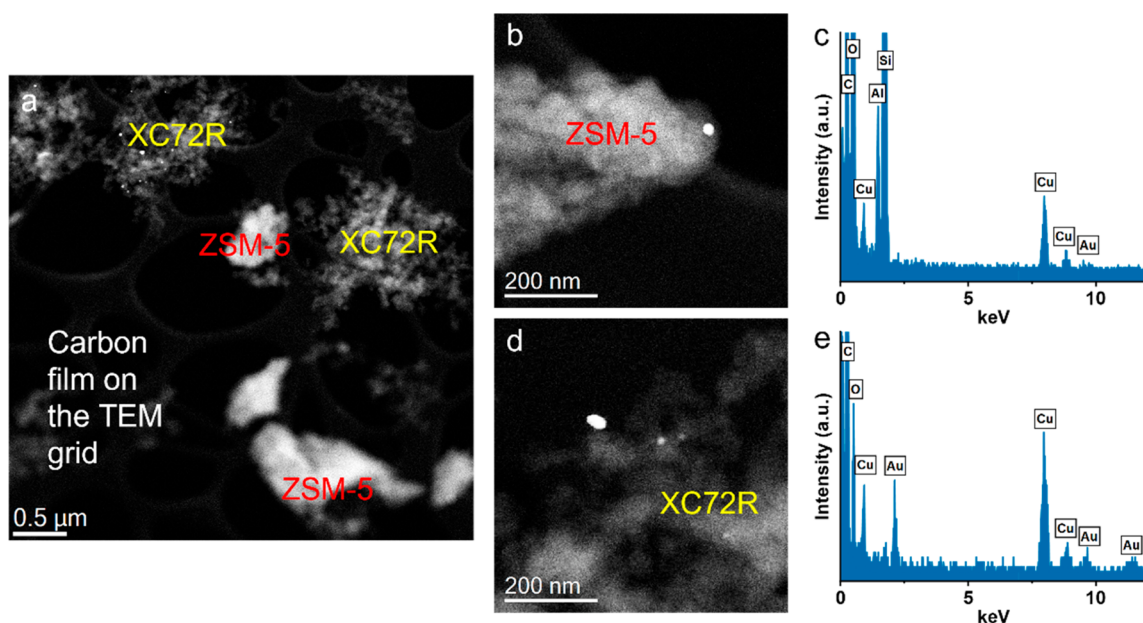


Figure 1. AC-STEM characterization of the Au/ZSM-5 and XC72R (0.08 g) catalyst after the methane oxidation reaction. (a) A lower magnification HAADF-STEM image, showing XC72R particles and ZSM-5 particles in the same field of view. (b, c) HAADF images and the corresponding X-ray energy dispersive spectrum of (b, c) a ZSM-5 particle and (d, e) a XC72R particle.

We subsequently conducted a series of methane oxidation studies utilizing a physical mixture of the Au/ZSM-5 catalyst and a range of carbon additives (Table 2, with textural properties of the carbons reported in Table S1). In a manner similar to that seen over the PVA-Au/ZSM-5 catalyst, a significant increase in both oxygenate productivity and CO₂ yield was observed, regardless of the carbon utilized. Notably, control experiments demonstrated that the increased production of methanol over the physical mixture systems was not a result of the separate activity of the individual components, i.e., the sum of the activities of separate experiments with Au/ZSM-5 and the carbon (with CH₄ + O₂) was considerably lower than when the Au/ZSM-5 and carbon were utilized together as a physical mixture. However, it is interesting to note that a significant proportion of acetic acid production (a minimum of 65% in all cases studied) may be attributed to the carbon additives (Table 2). XPS analysis of the fresh carbons (Table S2, Figure S2 and accompanying supplementary text) allows for the classification of the carbon additives into three categories of low, intermediate and high oxygen functionality. However, there is no clear relationship between the observed activity toward methanol (or total oxygenate) production and the extent of carbon oxidation that could be used to correlate the activities observed.

We subsequently set out to gain a greater understanding of the observed improvement in reactivity, with a particular focus on the physical mixture of Au/ZSM-5 and XC72R carbon, a material we have extensively investigated as a support for precious metal nanoparticles.³¹ Under an inert atmosphere or in the absence of O₂, negligible concentrations of oxygenates were detected over the XC72R carbon alone (Table 3, entries 1 and 2). However, upon the introduction of O₂, a significant amount of CO₂ was detected (Table 3, entry 3). By comparison, when the Au/ZSM-5 catalyst was utilized in the presence of O₂ and XC72R, but in the absence of methane (Table 3, entry 4), a relatively small amount of acetic acid was observed in addition to CO₂.

When CH₄ was reacted with O₂ in the presence of a physical mixture of Au/ZSM-5 and XC72R (Table 4, Figure S3), significant amounts of methanol were detected, over and above that observed over the Au/ZSM-5 catalyst alone (Table 4, entry 1). A strong correlation between the amount of XC72R utilized and oxygenate productivity was observed (Table 4, entries 2–6), although, notably, the effect on the yield of acetic acid was not very marked. In all cases and, perhaps unsurprisingly, given the contribution of the XC72R alone (Table 3), a pronounced enhancement in CO₂ production was also detected. Using XC72R as a support for the Au nanoparticles, with the catalyst prepared using an identical deposition procedure to that used for the Au/ZSM-5 analogue, led to an increase in the yield of methanol (Table 4, entry 7) compared to that observed over the Au/ZSM-5 catalyst alone. However, this was not as pronounced as that observed over a physical mixture of Au/ZSM-5 and XC72R, indicating that the zeolite plays an important role in the catalysis. Importantly, this experiment demonstrated that if any Au was transferred during the reaction from the ZSM-5 support to the carbon then it would not have a substantial effect on the observed reactivity. We investigated the possibility of such Au transfer using aberration-corrected microscopy. Selected catalysts were characterized using aberration-corrected scanning transmission electron microscopy (AC-STEM). Figure S4 shows the representative HAADF STEM images of the Au/ZSM-5 catalyst before and after use in the methane oxidation reaction. The Au nanoparticles can be clearly observed via the atomic number (Z) contrast. These STEM results suggest the catalysts mostly contain Au nanoparticles. Neither sub-nm nor atomically dispersed Au species were detected, which is consistent with our recent report.²³ The physical mixture of Au/ZSM-5 and XC72R (0.08 g) was also investigated after use in the methane oxidation reaction, via AC-STEM (Figure 1). Figure 1a shows a lower magnification HAADF-STEM image that has both ZSM-5 particles (brighter contrast) and XC72R particles (less bright contrast). Figure 1b–e shows HAADF-STEM

Table 5. Effect of Reaction Temperature on Methane Oxidation Using Au/ZSM-5 Catalyst in Addition to XC72R^a

Entry	Catalyst	Temperature (°C)	Productivity ($\mu\text{mol}/\text{g}_{\text{cat}}$)					CO ₂	Oxygenate selectivity (%)	Methanol selectivity in liquid (%)	Oxygenate productivity ($\mu\text{mol}/\text{g}_{\text{cat}}$)
			Methanol	Methyl hydroperoxide	Acetic acid	Peracetic acid					
1	Au/ZSM-5+XC72R	120	2.3	2.6	1.0	b.d.	6.9	50.0	33.3	5.9	
2	Au/ZSM-5	120	2.6	b.d.	2.8	1.2	2.8	79.1	24.5	6.6	
3	Au/ZSM-5+XC72R	160	8.5	b.d.	3.9	b.d.	44.8	26.7	52.2	12.4	
4	Au/ZSM-5	160	2.1	0.7	4.6	1.5	4.3	77.7	4.7	8.9	
5	Au/ZSM-5+XC72R	240	156	b.d.	13.0	b.d.	784	18.8	85.7	169	
6	Au/ZSM-5	240	9.72	0.6	7.5	3.3	20.0	61.4	30.4	21.1	

^aReaction conditions: Au/ZSM-5 (0.1 g), XC72R (0.08 g), H₂O (15 mL), 2 h, CH₄ (20.7 bar) and O₂ (3.5 bar) 1000 rpm. b.d.: below detection limit.

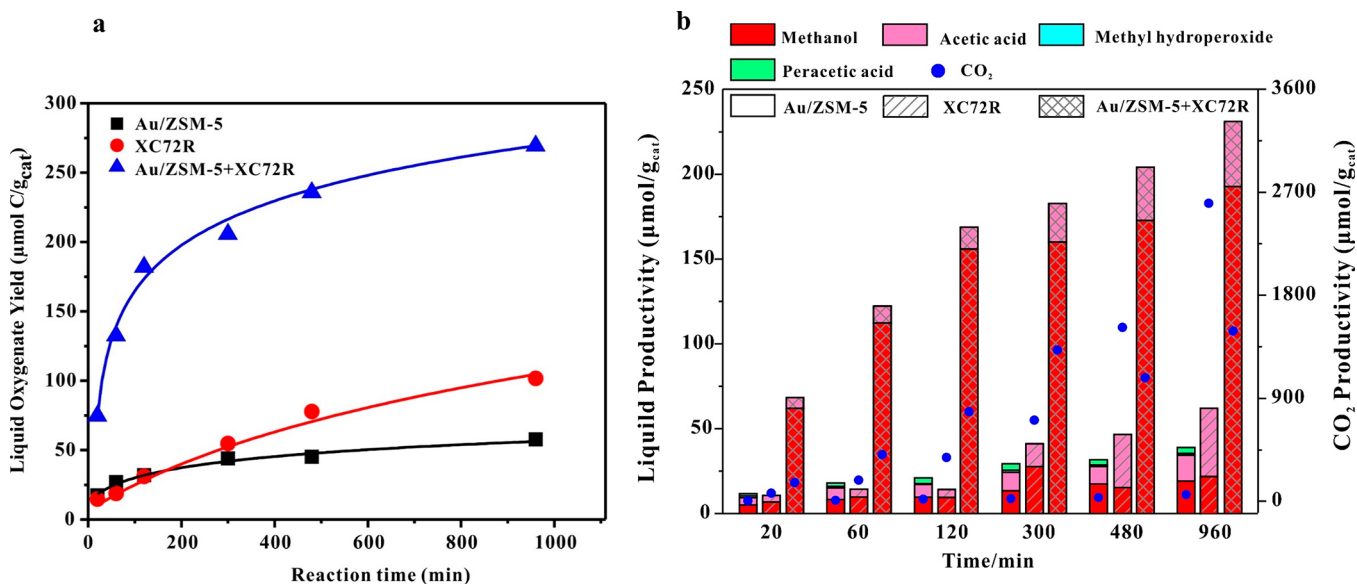


Figure 2. Promotional effect of XC72R addition on the catalytic performance of Au/ZSM-5, as a function of reaction time (a) total oxygenate yield, (b) liquid oxygenate and CO₂ productivity. Reaction conditions: Au/ZSM-5 (0.1 g), XC72R (0.08 g), H₂O (15 mL), 240 °C, CH₄ (20.7 bar), O₂ (3.5 bar), 1000 rpm.

Table 6. Influence of XC72R on the Analysis of Liquid Product in Methane Oxidation over Au/ZSM-5^a

Entry	Catalyst	Productivity ($\mu\text{mol}/\text{g}_{\text{cat}}$)					CO ₂	Oxygenate selectivity (%)	Methanol selectivity in liquid (%)	Oxygenate productivity ($\mu\text{mol}/\text{g}_{\text{cat}}$)
		Methanol	Methyl hydroperoxide	Acetic acid	Peracetic acid					
1	Au/ZSM-5	9.72	0.60	7.48	3.29	20.0	61.4	30.5	21.1	
2	Au/ZSM-5+XC72R (0.08 g)	9.71	0.56	7.48	b.d.	–	–	–	17.8	

^aStandard reaction conditions: Au/ZSM-5 (0.1 g), H₂O (15 mL), 240 °C, 2 h, 20.7 bar CH₄, 3.5 bar O₂, 1000 rpm. After a standard 2 h reaction over Au/ZSM-5 (entry 1), the reaction solution was split into two aliquots to one aliquot (entry 2), XC72R was added to the mixture and stirred for 10 min (1000 rpm at ambient conditions), then the liquid product was analyzed by ¹H NMR spectroscopy. b.d.: below detection limit.

images and the corresponding X-ray energy dispersive spectrum (X-EDS) of the two components. The presence of Au can be identified as bright particles on both the ZSM-5 and XC72R component in the HAADF-STEM images, with X-EDS analysis confirming the identity of the two support materials. The ZSM-5 support particle gave strong Al and Si X-ray signals (Figure 1c), which were absent from the XC72R particle (Figure 1e). These results strongly indicate that some of the Au species have migrated from the ZSM-5 support to the XC72R additive during the methane oxidation reaction and excludes any suggestion that the apparent migration of Au is an

artefact of the mode of analysis. However, it is important to note that the migration of Au from ZSM-5 to the XC72R is expected to lead to lower catalytic activity as explained earlier (Table 4, entry 7).

Further study demonstrated that the promotive effect of the carbon could be observed over a temperature range of at least 160–240 °C (Table 5). Comparisons of catalytic performance in the presence and absence of the XC72R additive over extended reaction times further highlights the relatively minor contribution from the carbon alone to liquid products (Figure 2a,b, Table S3). However, given the observed transfer of Au

Table 7. Influence of Reaction pH on the Methane Oxidation over a Physical Mixture of Au/ZSM-5 and XC72R^a

Entry	Catalyst	pH	Productivity ($\mu\text{mol/g}_{\text{cat}}$)					Oxygenate selectivity (%)	Methanol selectivity in liquid (%)	Oxygenate productivity ($\mu\text{mol/g}_{\text{cat}}$)
			Methanol	Methyl hydroperoxide	Acetic acid	Peracetic acid	CO ₂			
1	Au/ZSM-5	4 (HCl)	13.2	0.9	7.3	1.8	8.8	78.7	40.9	23.2
2		7	9.72	0.6	7.5	3.3	20.0	61.4	30.4	21.1
3		10 (NH ₃ ·H ₂ O)	3.2	1.1	6.1	2.4	3.8	85.0	15.0	12.7
4	Au/ZSM-5 + XC72R	4 (HCl)	129	b.d.	9.4	b.d.	386	27.7	87.3	138
5		7	156	b.d.	13.0	b.d.	784	18.8	85.7	169
6		10 (NH ₃ ·H ₂ O)	111	b.d.	14.7	b.d.	441	24.1	79.1	126

^aReaction conditions: Au/ZSM-5 (0.1 g), XC72R (0.08 g), H₂O (15 mL), 240 °C, 2 h, CH₄ (20.7 bar), O₂ (3.5 bar), 1000 rpm. The pH valve was adjusted by HCl or NH₃·H₂O. The pH of the solution in the autoclave was measured before reaction. b.d.: below detection limit.

Table 8. Effect of Sequential Gas Recharging on Methane Oxidation Activity^a

Entry	1st h	2nd h	Methanol	Productivity ($\mu\text{mol/g}_{\text{cat}}$)				Oxygenate selectivity (%)	Methanol selectivity in liquid (%)	Oxygenate productivity ($\mu\text{mol/g}_{\text{cat}}$)
				Methyl hydro peroxide	Acetic acid	Peracetic acid	CO ₂ ^b			
1	Au/ZSM-5	Au/ZSM-5	10.8	3.0	7.6	3.6	10.0 + 7.7 = 17.7	82.4	29.8	25.0
2	Au/ZSM-5	Au/ZSM-5 + XC72R	118	b.d.	12.7	b.d.	10.0 + 383 = 393	27.7	82.3	130
3	Au/ZSM-5	XC72R	11.4	b.d.	7.3	b.d.	10.0 + 227 = 237	9.9	43.9	18.7

^aReaction conditions: Au/ZSM-5 (0.1 g), XC72R (0.08 g), H₂O (15 mL), 240 °C, CH₄ (20.7 bar), O₂ (3.5 bar), 1000 rpm. All the reactions were reacted for 2 h. Au/ZSM-5 alone was used for the first hour, then the reaction was quenched by ice water to below 10 °C and gas products was collected. Entry 1: After an initial 1 h, reaction gaseous reagents were replaced and the reaction allowed to proceed for a further 1 h. Entry 2: After an initial 1 h reaction, XC72R (0.08 g) was introduced into the reactor, and gaseous reagents replaced. The reaction was allowed to proceed for a further 1 h. Entry 3: After an initial 1 h, reaction the Au/ZSM-5 catalyst was removed by centrifugation from the mixture. XC72R (0.08 g) was combined with the postreaction solution and reintroduced into the reactor, after the replacement of gaseous reagents the reaction was allowed to proceed for a further 1 h. b.d.: below detection limit. ^bCO₂: Sum of the CO₂ generated from the first hour (10 $\mu\text{mol/g}_{\text{cat}}$) and the second hour reactions.

between the ZSM-5 support and carbon additive (Figure 1), further study is still required in order to determine the effective lifetime of this system. Regardless the observed promotive effect achieved through carbon addition is noteworthy. As with our standard reaction (2 h), product yields obtained in the presence of a physical mixture of Au/ZSM-5 and XC72R were found to greatly exceed those observed when using either component alone. With the potential for XC72R to adsorb some of the products and therefore possibly mask the true extent of the observed effects a further experiment with the Au/ZSM-5 catalyst alone was conducted, as follows (Table 6). After the reaction, the postreaction mixture was cooled to room temperature and divided into two aliquots. The first was analyzed by ¹H NMR spectroscopy (Table 6, entry 1). To the second aliquot, XC72R (0.08 g) was added and the mixture stirred at ambient temperature for 10 min. Analysis of the second aliquot (Table 6, entry 2) demonstrated that XC72R did not affect the apparent product distribution, and hence product adsorption by the carbon can be discounted.

The effect of the reaction solution pH was subsequently investigated (Table 7) with the pH being adjusted between pH 4 and pH 10. A positive effect of adding XC72R was observed across the range of pH values investigated. In the case of the Au/ZSM-5 only experiments, an increase in reaction solution pH resulted in a decrease in the yield of oxygenated products, attributed to the partial dissolution of the ZSM-5 zeolite under more basic conditions, whereas when XC72R was present a maximum product yield was observed at pH 7.

A further set of experiments were conducted in which the Au/ZSM-5 catalyst was used to react CH₄ with O₂ under standard reaction conditions at 240 °C. After 1 h, the reaction was quenched using ice water to decrease the temperature below 10 °C and the gas products were collected. The gaseous reagents were replaced, and the reaction mixture was then subsequently reacted for a further 1 h (at 240 °C), in the presence of the Au/ZSM-5 catalyst and finally quenched and the products analyzed (Table 8, entry 1). In a separate reaction, XC72R was added to the second part of the reaction mixture (again with the retained Au/ZSM-5 catalyst) and similarly treated (Table 8, entry 2). In a third reaction mixture, the Au/ZSM-5 catalyst was removed by centrifugation, and XC72R was added and reacted for another 1 h (Table 8, entry 3). The production of CO₂ showed a marked increase when XC72R was added to the reaction mixture, in keeping with our earlier results (Table 2). However, only when both XC72R and Au/ZSM-5 were present did the methanol yield increase (Table 8, entry 2), while it was also demonstrated that that the XC72R carbon alone cannot facilitate the oxidation of methane under these reaction conditions (Table 8, entries 1 and 3). The addition of methanol at the start of the reaction in the presence of XC72R was found to have no effect, and hence under the reaction conditions, we have explored methanol is not reacted further by the carbon additive (Table S4).

Isotopically labeled ¹³CH₄ was used to determine the origin of the carbon in the methanol and CO₂ for the reaction when XC72R was added. The reaction data (Table S5) show that

within experimental error, identical liquid product profiles are observed for the reactions utilizing either $^{13}\text{CH}_4$ or CH_4 . For the reaction with CH_4 , the ^1H NMR signal of the methyl group

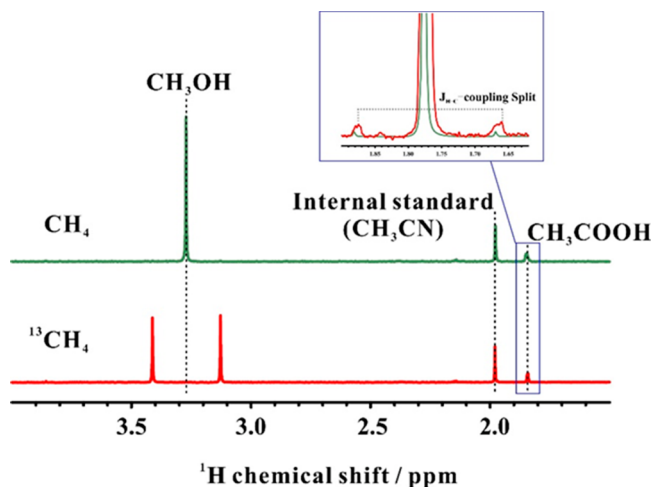


Figure 3. ^1H NMR spectra of the products obtained from the reactions using CH_4 in natural abundance or ^{13}C -labeled $^{13}\text{CH}_4$ as reactant. Insertion: Enlarged and normalized $J_{\text{H-C}}$ -coupling region of the methyl group of acetic acid.

in methanol occurs at 3.27 ppm (Figure 3). In comparison, the ^1H NMR signal of methanol for the reaction with $^{13}\text{CH}_4$ is completely split into a doublet at 3.41 and 3.13 ppm owing to the J -coupling of the proton with the ^{13}C atom in the methyl group. This result supports our earlier investigations into the contribution of the carbon alone to the observed catalysis, with the negligible formation of methanol in the absence of the Au/ZSM-5 catalyst (Table 2, Table S2). Such studies indicate that the vast majority of the carbon in the methanol originates from CH_4 . Likewise, based on these isotopically labeled experiments, we were also able to determine that the carbon additive is the primary source of acetic acid. Mass spectrometry analysis (Figure 4) shows that about 61.5% CO_2 originates from $^{13}\text{CH}_4$ and 38.5% from XC72R as determined by the comparison of the peak intensity of $^{13}\text{CO}_2$ and CO_2 obtained from the reaction using $^{13}\text{CH}_4$.

The experiment using ^{13}C -labeled methane helps to explain the origin of the marked enhancement in oxygenate production when carbon is used in conjunction with the Au/ZSM-5 catalysts. As the enhancement in methanol yield results almost entirely from the increased reaction of methane, it is apparent that the added carbon is not catalytically active and instead acts as a promoter for Au/ZSM-5.

We consider that, when used in conjunction with the Au/ZSM-5 catalyst, the carbon may act as a reducing agent and promote the formation of active oxo-species on the metal surface; however, the degree to which the Au/ZSM-5 catalyst and partially oxidized carbon additive must be in intimate contact for such a promotion to be achieved is still unclear.^{22,30} Regardless, this observed enhancement is similar to the effect of adding CO as a reactant which has been well-reported to enhance the rate of oxidation of hydrocarbons over zeolite-supported metal catalysts.^{11,23,32}

To determine the mechanism by which the carbon additive exerts its effect on the observed catalytic reaction, we subsequently carried out further experiments. First, as it is known that hydrogen peroxide can be an effective oxidant and it is possible that surface species on the carbon could be an effective source of hydrogen for hydrogen peroxide synthesis, we, therefore, analyzed the reaction mixture of Au/ZSM-5 with $\text{CH}_4 + \text{O}_2$ with XC72R and no hydrogen peroxide was observed. Next, we investigated whether it is the formation of gas phase CO, a well-reported promoter for supported metal-mediated methane activation,^{11,23,32} as a reaction intermediate that is the origin of the effect. In the reaction of $\text{CH}_4 + \text{O}_2$ with Au/ZSM-5 in the presence of carbon, no gas phase CO is observed in the product stream (Figure S5). We then added CO to the reaction gases, and even when added in low amounts, the CO was not totally consumed (Table 9). Therefore, we conclude that the formation of CO released from the surface of the carbon as a reaction intermediate is not the source of the observed promotion. However, the promotive effect of adding carbon to the reaction mixture (Table 4) is similar to that of adding CO as both show a linear relationship between the enhancement in activity and the amount of carbon or CO added (Figure S6). An early study by Nelson Smith and co-workers³³ showed that the surface of carbon can be oxidized and functionalized by reaction with water at 200 °C, a temperature very similar to that used in our study. With this earlier work in mind and in an attempt to determine the

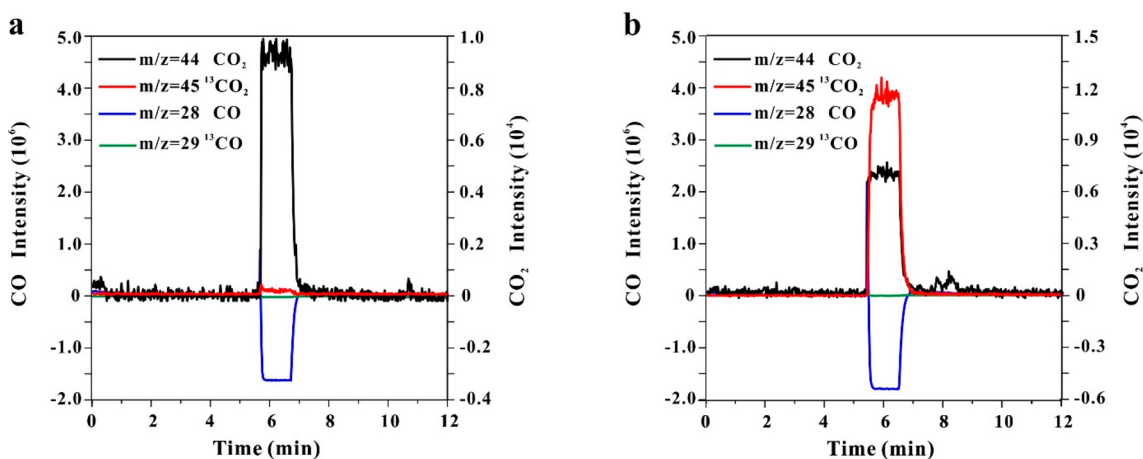


Figure 4. Mass spectrometry analysis of gas products obtained from the reactions using (a) $^{12}\text{CH}_4$ and (b) $^{13}\text{CH}_4$ as reactant.

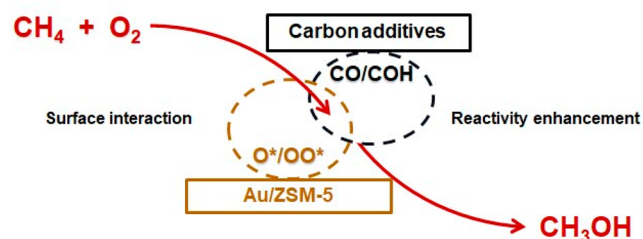
Table 9. CH₄ Oxidation on Au/ZSM-5 Catalysts^a

Entry	Reactants CH ₄ , CO, O ₂ (bar)	Productivity (μmol/g _{cat})					Added CO (μmol)	Residual CO (μmol)	CO conversion (%) ^b	Oxygenate selectivity (%)	Methanol selectivity in liquid (%)	Oxygenate productivity (μmol/g _{cat})
		Methanol	Methyl hydroperoxide	Acetic acid	Peracetic acid	CO ₂						
1	20.7, 0, 3.5	8.2	0.8	7.0	2.0	9.9	0.0	0.0	0.0	73.1	30.4	18.0
2	23.06, 0.14, 1	67.5	0.3	8.1	2.3	199.3	84.7	65.3	22.8	30.7	76.4	78.1
3	22.7, 0.5, 1	134.2	0.0	11.3	2.6	706.3	302.4	224.1	25.9	18.7	82.8	148.1
4	22.2, 1, 1	233.3	0.0	21.9	3.2	1289.6	604.8	505.2	16.5	18.0	82.4	258.3

^aReaction conditions: Catalyst (0.1 g), H₂O (15 mL), 240 °C, 1 h, 1000 rpm. ^bCO conversion (%) = (added CO – residual CO)/(added CO) × 100%.

chemical stability of the XC72R additive, we subsequently carried out detailed TPO studies of the XC72R carbon, with the as-received material observed to undergo oxidation at approximately 595 °C, with no significant variation observed for analogous samples after exposure to methane oxidation reaction conditions (Figure S7). However, additional XPS measurements of the fresh XC72R carbon and the same carbon after use in the methane oxidation reaction (in water at 240 °C) do indeed show that the surface of the carbon has been oxidized (Figure S8), with a clear increase in C–O/C–OH functionality observed after exposure to reaction conditions. We consider that it is the oxidized surface of the carbon that is the source of the enhancement in reaction that we observe (Scheme 1). In our recent paper³¹ we reported that the

Scheme 1. Schematic Illustration on the Promotive Effect of Carbon Additives on the Methane Oxidation Catalyzed by Au/ZSM-5



addition of XC72R to a physical mixture of Au/TiO₂ and Pd/TiO₂ in an aqueous reaction mixture enhanced the oxidation of an alcohol. This we considered to be due to a new cooperative enhancement effect which is ascribed to electron transfer between the Au and Pd aided by the conductivity of the XC72R. This shows that XC72R can readily interact with a supported Au catalyst when added as a physical mixture. Taking these observations as a whole, we now conclude that the effect we observe of the enhancement in methane oxidation with Au/ZSM-5 as a catalyst when XC72R is added is due to the surface of the XC72R being oxidized by water/O₂ at elevated reaction temperatures and it is this oxidized carbon surface interacting with the Au/ZSM-5 that facilitates the enhanced activity observed. Although we cannot rule out the involvement of a reducing species, for example, formaldehyde, transferring between the carbon and Au/ZSM-5, notably we do not observe any new liquid phase species in the presence of added carbon. We therefore postulate a direct interaction between the surfaces of the two materials and the surface species present upon them. These may include CO as an adsorbed species on the carbon, but it does not desorb. Hence,

we consider that the mechanism by which carbon acts in this reaction is not via the formation of gas phase CO in situ as a reaction intermediate, rather carbon and CO exert similar effects but do so via by different routes.

The reactivity of carbon in water at 240 °C in the oxidation of methane is an unexpected finding. Indeed, the oxidation of carbon when methane is present occurs at temperatures as low as 120 °C. It is possible that this observation may have some relevance to the design of catalysts with reduced coking during the oxidation of hydrocarbons.

CONCLUSION

The addition of a range of carbon additives to a Au/ZSM-5 catalyst has been shown to significantly enhance catalytic performance toward the oxidation of methane, when using O₂ as the terminal oxidant. The reaction produces both methanol and acetic acid as products together with CO₂. Notably, ¹³C labelling studies show that while a considerable proportion of acetic acid production observed can be attributed to the carbon additive, the direct contribution of the carbon promoters to methanol formation is negligible. Indeed, our studies indicate that the carbon materials alone are not directly responsible for the observed improvement in oxygenate production and rather they act as a promoter for the Au/ZSM-5 catalyst. Notably, no direct correlation may be drawn between the extent of catalytic promotion and criteria such as surface area, purity or functionality of the as-received carbons. Rather, we attribute the observed enhancement in catalytic performance to the partial oxidation of the surface of the carbon, and it is the interaction of the oxidized carbon surface with the Au/ZSM-5 catalyst that is responsible for the observed improvement in catalytic performance. The presence of water is key in achieving the partial oxidation of the carbon additives at temperatures far lower than that which may be expected based on temperature programmed oxidation analysis of the pristine carbon materials.

ASSOCIATED CONTENT

Supporting Information

The Supporting Information is available free of charge at <https://pubs.acs.org/doi/10.1021/acscatal.3c01226>.

Data relating to catalytic activity toward the selective oxidation of methane, with accompanying characterization of catalytic materials and carbon promoters via TGA, XPS, HAADF-STEM, TPO as well as porosimetry analysis and surface area determination (PDF)

■ AUTHOR INFORMATION

Corresponding Authors

Graham J. Hutchings – Max Planck–Cardiff Centre on the Fundamentals of Heterogeneous Catalysis FUNCAT, Cardiff Catalysis Institute, School of Chemistry, Cardiff University, Cardiff CF10 3AT, United Kingdom; orcid.org/0000-0001-8885-1560; Email: Hutch@cardiff.ac.uk

Jun Xu – National Centre for Magnetic Resonance in Wuhan, State Key Laboratory of Magnetic Resonance and Atomic and Molecular Physics, Innovation Academy for Precision Measurement Science and Technology, Chinese Academy of Sciences, Wuhan 430071, China; University of Chinese Academy of Sciences, Beijing 100049, China; orcid.org/0000-0003-2741-381X; Email: xujun@wipm.ac.cn

Authors

Jingxian Cao – National Centre for Magnetic Resonance in Wuhan, State Key Laboratory of Magnetic Resonance and Atomic and Molecular Physics, Innovation Academy for Precision Measurement Science and Technology, Chinese Academy of Sciences, Wuhan 430071, China; University of Chinese Academy of Sciences, Beijing 100049, China

Richard J. Lewis – Max Planck–Cardiff Centre on the Fundamentals of Heterogeneous Catalysis FUNCAT, Cardiff Catalysis Institute, School of Chemistry, Cardiff University, Cardiff CF10 3AT, United Kingdom; orcid.org/0000-0001-9990-7064

Guodong Qi – National Centre for Magnetic Resonance in Wuhan, State Key Laboratory of Magnetic Resonance and Atomic and Molecular Physics, Innovation Academy for Precision Measurement Science and Technology, Chinese Academy of Sciences, Wuhan 430071, China; University of Chinese Academy of Sciences, Beijing 100049, China

†Donald Bethell – Max Planck–Cardiff Centre on the Fundamentals of Heterogeneous Catalysis FUNCAT, Cardiff Catalysis Institute, School of Chemistry, Cardiff University, Cardiff CF10 3AT, United Kingdom

Mark J. Howard – Max Planck–Cardiff Centre on the Fundamentals of Heterogeneous Catalysis FUNCAT, Cardiff Catalysis Institute, School of Chemistry, Cardiff University, Cardiff CF10 3AT, United Kingdom

Brian Harrison – Max Planck–Cardiff Centre on the Fundamentals of Heterogeneous Catalysis FUNCAT, Cardiff Catalysis Institute, School of Chemistry, Cardiff University, Cardiff CF10 3AT, United Kingdom

Bingqing Yao – National University of Singapore, Singapore 117575, Singapore

Qian He – National University of Singapore, Singapore 117575, Singapore; orcid.org/0000-0003-4891-3581

David J. Morgan – Max Planck–Cardiff Centre on the Fundamentals of Heterogeneous Catalysis FUNCAT, Cardiff Catalysis Institute, School of Chemistry, Cardiff University, Cardiff CF10 3AT, United Kingdom; orcid.org/0000-0002-6571-5731

Fenglou Ni – Max Planck–Cardiff Centre on the Fundamentals of Heterogeneous Catalysis FUNCAT, Cardiff Catalysis Institute, School of Chemistry, Cardiff University, Cardiff CF10 3AT, United Kingdom

Pankaj Sharma – School of Chemistry, Cardiff University, Cardiff CF10 3AT, United Kingdom; UK Catalysis Hub, Research Complex at Harwell, Rutherford Appleton Laboratory, Harwell OX11 0FA, United Kingdom; orcid.org/0000-0003-2319-260X

Christopher J. Kiely – Department of Materials Science and Engineering, Lehigh University, Bethlehem, Pennsylvania 18015, United States

Xu Li – National Centre for Magnetic Resonance in Wuhan, State Key Laboratory of Magnetic Resonance and Atomic and Molecular Physics, Innovation Academy for Precision Measurement Science and Technology, Chinese Academy of Sciences, Wuhan 430071, China; University of Chinese Academy of Sciences, Beijing 100049, China

Feng Deng – National Centre for Magnetic Resonance in Wuhan, State Key Laboratory of Magnetic Resonance and Atomic and Molecular Physics, Innovation Academy for Precision Measurement Science and Technology, Chinese Academy of Sciences, Wuhan 430071, China; University of Chinese Academy of Sciences, Beijing 100049, China; orcid.org/0000-0002-6461-7152

Complete contact information is available at: <https://pubs.acs.org/10.1021/acscatal.3c01226>

Notes

The authors declare no competing financial interest.

[†]Deceased December 4, 2022.

■ ACKNOWLEDGMENTS

This work was financially supported by the National Key R&D Program of China (2022YFA1504500) and the National Natural Science Foundation of China (U1932218, 22225205, 22127801). J.X. thanks the Royal Society and the Newton Fund for Royal Society-Newton Advanced Fellowship (NAF\R1\201066). G.J.H. acknowledges the support from the Chinese Academy of Sciences (CAS) President's International Fellowship Initiative (PIFI) (grant no. 2019DM0015). Q.H. thanks the support from National Research Foundation (NRF) Singapore, under its NRF Fellowship (NRF-NRFF11-2019-0002). R.J.L. and G.J.H. thank Cardiff University and the Max Planck Centre for Fundamental Heterogeneous Catalysis (FUNCAT) for financial support. XPS data collection was performed at the EPSRC National Facility for XPS ("HarwellXPS"), operated by Cardiff University and UCL, under contract no. PR16195.

■ REFERENCES

- (1) Dummer, N. F.; Willock, D. J.; He, Q.; Howard, M. J.; Lewis, R. J.; Qi, G.; Taylor, S. H.; Xu, J.; Bethell, D.; Kiely, C. J.; Hutchings, G. J. Methane Oxidation to Methanol. *Chem. Rev.* **2022**, DOI: [10.1021/acs.chemrev.2c00439](https://doi.org/10.1021/acs.chemrev.2c00439).
- (2) Periana, R. A.; Taube, D. J.; Evitt, E. R.; Loffler, D. G.; Wentrcck, P. R.; Voss, G.; Masuda, T. A Mercury-Catalyzed, High-Yield System for the Oxidation of Methane to Methanol. *Science* **1993**, *259*, 340–343.
- (3) Periana, R. A.; Taube, D. J.; Gamble, S.; Taube, H.; Satoh, T.; Fujii, H. Platinum catalysts for the high-yield oxidation of methane to a methanol derivative. *Science* **1998**, *280*, 560–564.
- (4) Sobolev, V. I.; Dubkov, K. A.; Panna, O. V.; Panov, G. I. Selective Oxidation of Methane to Methanol on a FeZsm-5 Surface. *Catal. Today* **1995**, *24*, 251–252.
- (5) Starokon, E. V.; Parfenov, M. V.; Pirutko, L. V.; Abornev, S. I.; Panov, G. I. Room-Temperature Oxidation of Methane by α -Oxygen and Extraction of Products from the FeZSM-5 Surface. *J. Phys. Chem. C* **2011**, *115*, 2155–2161.
- (6) Starokon, E. V.; Parfenov, M. V.; Arzumanov, S. S.; Pirutko, L. V.; Stepanov, A. G.; Panov, G. I. Oxidation of methane to methanol on the surface of FeZSM-5 zeolite. *J. Catal.* **2013**, *300*, 47–54.

- (7) Parfenov, M. V.; Starokon, E. V.; Pirutko, L. V.; Panov, G. I. Quasicatalytic and catalytic oxidation of methane to methanol by nitrous oxide over FeZSM-5 zeolite. *J. Catal.* **2014**, *318*, 14–21.
- (8) Hammond, C.; Forde, M. M.; Ab Rahim, M. H.; Thetford, A.; He, Q.; Jenkins, R. L.; Dimitratos, N.; Lopez-Sanchez, J. A.; Dummer, N. F.; Murphy, D. M.; et al. Direct catalytic conversion of methane to methanol in an aqueous medium by using copper-promoted Fe-ZSM-5. *Angew. Chem.* **2012**, *124*, 5219–5223.
- (9) Yu, T.; Li, Z.; Lin, L.; Chu, S.; Su, Y.; Song, W.; Wang, A.; Weckhuysen, B. M.; Luo, W. Highly selective oxidation of methane into methanol over Cu-promoted monomeric Fe/ZSM-5. *ACS Catal.* **2021**, *11*, 6684–6691.
- (10) Narsimhan, K.; Michaelis, V. K.; Mathies, G.; Gunther, W. R.; Griffin, R. G.; Roman-Leshkov, Y. Methane to acetic acid over Cu-exchanged zeolites: mechanistic insights from a site-specific carbonylation reaction. *J. Am. Chem. Soc.* **2015**, *137*, 1825–1832.
- (11) Shan, J.; Li, M.; Allard, L. F.; Lee, S.; Flytzani-Stephanopoulos, M. Mild oxidation of methane to methanol or acetic acid on supported isolated rhodium catalysts. *Nature* **2017**, *551*, 605–608.
- (12) Tang, Y.; Li, Y.; Fung, V.; Jiang, D.-e.; Huang, W.; Zhang, S.; Iwasawa, Y.; Sakata, T.; Nguyen, L.; Zhang, X.; et al. Single rhodium atoms anchored in micropores for efficient transformation of methane under mild conditions. *Nat. Commun.* **2018**, *9*, 1–11.
- (13) Jin, Z.; Wang, L.; Zuidema, E.; Mondal, K.; Zhang, M.; Zhang, J.; Wang, C.; Meng, X.; Yang, H.; Mesters, C.; et al. Hydrophobic zeolite modification for in situ peroxide formation in methane oxidation to methanol. *Science* **2020**, *367*, 193–197.
- (14) Agarwal, N.; Freakley, S. J.; McVicker, R. U.; Althabhan, S. M.; Dimitratos, N.; He, Q.; Morgan, D. J.; Jenkins, R. L.; Willock, D. J.; Taylor, S. H.; et al. Aqueous Au-Pd colloids catalyze selective CH₄ oxidation to CH₃OH with O₂ under mild conditions. *Science* **2017**, *358*, 223–227.
- (15) Groothaert, M. H.; Smeets, P. J.; Sels, B. F.; Jacobs, P. A.; Schoonheydt, R. A. Selective oxidation of methane by the bis (μ -oxo) dicopper core stabilized on ZSM-5 and mordenite zeolites. *J. Am. Chem. Soc.* **2005**, *127*, 1394–1395.
- (16) Tomkins, P.; Mansouri, A.; Bozbag, S. E.; Krumeich, F.; Park, M. B.; Alayon, E. M. C.; Ranocchiaro, M.; van Bokhoven, J. A. Isothermal cyclic conversion of methane into methanol over copper-exchanged zeolite at low temperature. *Angew. Chem.* **2016**, *128*, 5557–5561.
- (17) Grundner, S.; Markovits, M. A.; Li, G.; Tromp, M.; Pidko, E. A.; Hensen, E. J.; Jentys, A.; Sanchez-Sanchez, M.; Lercher, J. A. Single-site trinuclear copper oxygen clusters in mordenite for selective conversion of methane to methanol. *Nat. Commun.* **2015**, *6*, 1–9.
- (18) Sushkevich, V. L.; Palagin, D.; Ranocchiaro, M.; Van Bokhoven, J. A. Selective anaerobic oxidation of methane enables direct synthesis of methanol. *Science* **2017**, *356*, 523–527.
- (19) Narsimhan, K.; Iyoki, K.; Dinh, K.; Román-Leshkov, Y. Catalytic oxidation of methane into methanol over copper-exchanged zeolites with oxygen at low temperature. *ACS central science* **2016**, *2*, 424–429.
- (20) Dinh, K. T.; Sullivan, M. M.; Narsimhan, K.; Serna, P.; Meyer, R. J.; Dincă, M.; Román-Leshkov, Y. Continuous partial oxidation of methane to methanol catalyzed by diffusion-paired copper dimers in copper-exchanged zeolites. *J. Am. Chem. Soc.* **2019**, *141*, 11641–11650.
- (21) Koishybay, A.; Shantz, D. F. Water is the oxygen source for methanol produced in partial oxidation of methane in a flow reactor over Cu-SSZ-13. *J. Am. Chem. Soc.* **2020**, *142*, 11962–11966.
- (22) Hashmi, A. S. K.; Hutchings, G. J. Gold Catalysis. *Angew. Chem., Int. Ed.* **2006**, *45*, 7896–7936.
- (23) Qi, G.; Davies, T. E.; Nasrallah, A.; Sainna, M. A.; Howe, A. G.; Lewis, R. J.; Quesne, M.; Catlow, C. R. A.; Willock, D. J.; He, Q.; et al. Au-ZSM-5 catalyses the selective oxidation of CH₄ to CH₃OH and CH₃COOH using O₂. *Nat. Catal.* **2022**, *5*, 45–54.
- (24) Cooper, C.; Wiezevich, P. Effects of temperature and pressure on the upper explosive limit of methane-oxygen mixtures. *Ind. Eng. Chem.* **1929**, *21*, 1210–1214.
- (25) Hummers, W. S.; Offeman, R. E. Preparation of Graphitic Oxide. *J. Am. Chem. Soc.* **1958**, *80*, 1339–1339.
- (26) Pattison, S.; Nowicka, E.; Gupta, U. N.; Shaw, G.; Jenkins, R. L.; Morgan, D. J.; Knight, D. W.; Hutchings, G. J. Tuning graphitic oxide for initiator- and metal-free aerobic epoxidation of linear alkenes. *Nat. Commun.* **2016**, *7*, 12855.
- (27) Fairley, N.; Fernandez, V.; Richard-Plouet, M.; Guillot-Deudon, C.; Walton, J.; Smith, E.; Flahaut, D.; Greiner, M.; Biesinger, M.; Tougaard, S.; Morgan, D.; Baltrusaitis, J. Systematic and collaborative approach to problem solving using X-ray photoelectron spectroscopy. *Appl. Sur. Sci. Adv.* **2021**, *5*, 100112.
- (28) Scofield, J. H. Hartree-Slater subshell photoionization cross-sections at 1254 and 1487 eV. *J. Electron Spectrosc.* **1976**, *8*, 129–137.
- (29) Tanuma, S.; Powell, C. J.; Penn, D. R. Calculations of electron inelastic mean free paths. V. Data for 14 organic compounds over the 50–2000 eV range. *Surf. Interface Anal.* **1994**, *21*, 165–176.
- (30) Forde, M. M.; Grazia, B. C.; Armstrong, R.; Jenkins, R. L.; Ab Rahim, M. H.; Carley, A. F.; Dimitratos, N.; Lopez-Sanchez, J. A.; Taylor, S. H.; McKeown, N. B.; et al. Methane oxidation using silica-supported N-bridged di-iron phthalocyanine catalyst. *J. Catal.* **2012**, *290*, 177–185.
- (31) Huang, X.; Akdim, O.; Douthwaite, M.; Wang, K.; Zhao, L.; Lewis, R. J.; Pattison, S.; Daniel, I. T.; Miedziak, P. J.; Shaw, G.; et al. Au-Pd separation enhances bimetallic catalysis of alcohol oxidation. *Nature* **2022**, *603*, 271–275.
- (32) Moteki, T.; Tominaga, N.; Ogura, M. CO-Assisted Direct Methane Conversion into C1 and C2 Oxygenates over ZSM-5 Supported Transition and Platinum Group Metal Catalysts Using Oxygen as an Oxidant. *ChemCatChem* **2020**, *12*, 2957–2961.
- (33) Smith, R. N.; Pierce, C.; Joel, C. D. The low temperature reaction of water with carbon. *J. Phys. Chem.* **1954**, *58*, 298–302.

Recommended by ACS

Ultrathin TiO_x Nanosheets Rich in Tetracoordinated Ti Sites for Propane Dehydrogenation

Yiyi Xu, Jinlong Gong, et al.

APRIL 19, 2023
ACS CATALYSIS

READ 

Thermal Aging of Rh/ZrO₂-CeO₂ Three-Way Catalysts under Dynamic Lean/Rich Perturbation Accelerates Deactivation via an Encapsulation Mechanism

Masato Machida, Masayuki Tsushida, et al.

MARCH 03, 2023
ACS CATALYSIS

READ 

Empowering Catalyst Supports: A New Concept for Catalyst Design Demonstrated in the Fischer-Tropsch Synthesis

Motlokoa Khasu, Nico Fischer, et al.

MAY 04, 2023
ACS CATALYSIS

READ 

Support-Dependent Activity and Thermal Stability of Ru-Based Catalysts for Catalytic Combustion of Light Hydrocarbons

Hangqi Xia, Qiguang Dai, et al.

JANUARY 23, 2023
INDUSTRIAL & ENGINEERING CHEMISTRY RESEARCH

READ 

Get More Suggestions >